



LAWRENCE
LIVERMORE
NATIONAL
LABORATORY

Modeling of light intensification by conical pits within multilayer coatings

S. R. Qiu, J. E. Wolfe, A. Monterrosa, M. D. Feit,
T. V. Pistor, C. J. Stolz

November 16, 2009

Boulder Damage Symposium
Boulder, CO, United States
September 21, 2009 through September 23, 2009

Disclaimer

This document was prepared as an account of work sponsored by an agency of the United States government. Neither the United States government nor Lawrence Livermore National Security, LLC, nor any of their employees makes any warranty, expressed or implied, or assumes any legal liability or responsibility for the accuracy, completeness, or usefulness of any information, apparatus, product, or process disclosed, or represents that its use would not infringe privately owned rights. Reference herein to any specific commercial product, process, or service by trade name, trademark, manufacturer, or otherwise does not necessarily constitute or imply its endorsement, recommendation, or favoring by the United States government or Lawrence Livermore National Security, LLC. The views and opinions of authors expressed herein do not necessarily state or reflect those of the United States government or Lawrence Livermore National Security, LLC, and shall not be used for advertising or product endorsement purposes.

Modeling of light intensification by conical pits within multilayer high reflector coatings

S. Roger Qiu^{a*}, Justin E. Wolfe^a, Anthony M. Monterrosa^b, Michael D. Feit^a, Thomas V. Pistor^c,
Christopher J. Stolz^a

^a*Lawrence Livermore National Laboratory, 7000 East Avenue, Livermore, CA 94551*

^b*Department of Nuclear Engineering and Department of Materials Science & Engineering,
University of California, Berkeley, CA 94704*

^c*Panoramic Technology Inc., 2039 Shattuck Ave., Suite 404, Berkeley, CA 94704*

ABSTRACT

Removal of laser-induced damage sites provides a possible mitigation pathway to improve damage resistance of coated multilayer dielectric mirrors. In an effort to determine the optimal mitigation geometry which will not generate secondary damage precursors, the electric field distribution within the coating layers for a variety of mitigation shapes under different irradiation angles has been estimated using the finite difference time domain (FDTD) method. The coating consists of twenty-four alternating layers of hafnia and silica with a quarter-wave reflector design. A conical geometrical shape with different cone angles is investigated in the present study. Beam incident angles range from 0° to 60° at 5° increments. We find that light intensification (square of electric field, $|\mathbf{E}|^2$) within the multilayers depends strongly on the beam incident direction and the cone angle. By comparing the field intensification for each cone angle under all angles of incidence, we find that a 30° conical pit generates the least field intensification within the multilayer film. Our results suggest that conical pits with shallow cone angles ($\leq 30^\circ$) can be used as potential optimal mitigation structures.

Keywords: Laser-induced damage, mitigation, QWOT, conical pit, FDTD, light intensification, multilayer coating.

1. INTRODUCTION

Silica-Hafnia multilayer coatings are often used on mirrors on high peak power laser systems like the National Ignition Facility. The high dielectric constant multilayers are coated on BK7 substrates by physical vapor deposition. Defects are inevitably formed during the deposition process within the film as well as on the surface of the outer-most layers. Some rare defects such as the highly absorbing nano-clusters at the near surface region of the film, or the solid inclusions in the bulk can result in damage upon exposure to laser light.¹⁻² Earlier studies have shown that substrate scratches and impurities can also contribute to laser damage of the coating layers.³ Because some of these initiated sites grow at higher fluences, they limit the lifetime as well as the performance of mirrors.

One of the strategies to minimize laser damage and enhance mirror performance is first to initiate the damage precursors at lower fluences, and then replace the initiated damage sites with pre-designed mitigation structures⁴. These mitigation structures can be created by multiple techniques including femtosecond laser machining, single crystal high-speed diamond machining, and magnetorheological finishing.⁴⁻⁶ The challenge is to determine the proper mitigation structure which will not induce subsequent damage at operational fluence. Since electric field peaks exceeding the intrinsic standing-wave peaks are often created within multilayer coatings owing to interface and coating defects,⁷ the initiation of laser damage within optical coatings due to defective structures can be better understood by electric field modeling.⁸ In this paper, we report 2-D modeling results on light intensification within multilayer coating layers due to conical pits of various cone angles at different irradiation conditions. We find that a 30° conical pit generates the least field intensification and thus can be used as a potential mitigation structure.

2. METHOD AND VALIDATION

The modeling of light intensification within multilayer film due to defective structures is achieved by utilizing a commercially available software code TEMPESTpr2.⁹⁻¹⁰ TEMPESTpr2 employs a finite difference time domain (FDTD) method¹¹ to solve Maxwell's equations within a particular structure, both in 2-D and 3-D. The algorithm for this study simulates the scattering of an electromagnetic plane wave by using a defective multilayer mirror topography. The simulation domain is rectangular, 2-D, and gridded with a uniform grid. In the original code, the periodic boundary conditions (PBC) are applied in the horizontal (or the x) direction, while the Berenger's perfectly matched layer (PML) absorbing-boundary condition¹² is applied in the vertical (or the z) direction.

An earlier version of the program TEMPESTpr1 has been used to study the electric field enhancement by spherical inclusions embedded within multilayer coatings^{8, 13-14} and by cracks within fused silica surfaces.¹⁵ The simulation results provided explanations for the experimental observations. In the current study, we expand the capability to examine the field intensification within a multilayer film that contains conical pits of different cone angles. Here we report 2-D simulation results for cone angles of 0°, 30°, 45°, 60° and 80° and the incidence angles of 0° to 60° in 5° increments.

Figure 1 illustrates the defect geometry used in this study. The simulation domain is 90 μm wide and 4.963 μm high (unless otherwise noted) and contains 24 alternating layers of hafnia (H) and silica (L) with a quarter-wave reflector design: air:L(L:H)¹²:glass. A conical pit of 30° cone angle defect is inscribed within the domain on the surface of a BK7 glass substrate. For normal incidence irradiation, the reference wavelength is 1053 nm, and the refractive indices of the layers are $n_H=1.971$ and $n_L=1.44977$. The physical thickness of each hafnia and silica layer is 133.56 and 181.58 nm, respectively. The total film thickness is 3963.26 nm. For oblique incidence cases, the irradiation wavelength for the calculations was blue-shifted to maintain maximum reflectivity and proper spectral centering; the refractive indices were replaced by the effective values as discussed in later sections.

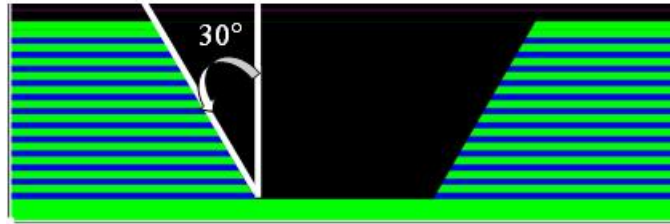


Figure 1. Example of the simulation domain for a multilayer coating with a conical defect of 30° cone angle on a glass substrate.

There are some inherent errors in film thickness when discretizing the layer structure during the simulation since uniform gridding is required. An example of the gridding to the film thickness is shown in figure 2a. Figure 2b shows the layer thickness errors as a function of cells per bilayer for normal incidence. As indicated in the plot, to achieve an error less than 2%, the number of cells per bilayer can be 7, 12, 14, or 19. Since the computer memory usage and simulation time are directly proportional to the number of cells in the simulation domain, 12 cells per bilayer (7 cells for SiO₂ and 5 cells for HfO₂) is chosen for our simulation to balance the simulation accuracy and computing time. Furthermore, the 12 cells per bilayer also give a smaller error in thickness for oblique incidences (figure 2c). As indicated earlier, for oblique incidence cases, we also corrected the incident wavelength to account for angle-induced spectral shifting. The adjusted wavelength for each incident angle is calculated using "The Essential Macleod" program¹⁶, a comprehensive software package for the design and analysis of optical thin film. To further overcome the ± quarter wave optical thickness (QWOT) error, effective indices of refraction are used. The modification to the index of refraction is given by the following formula

$$n(\text{HfO}_2) = 2.0058 - 0.0002 * \theta - 0.00003 * \theta^2$$

$$n(\text{SiO}_2) = 1.4316 + 0.0001 * \theta + 0.00005 * \theta^2$$

where θ is the angle of incidence. The correction is within 2% of the original indices of each material.

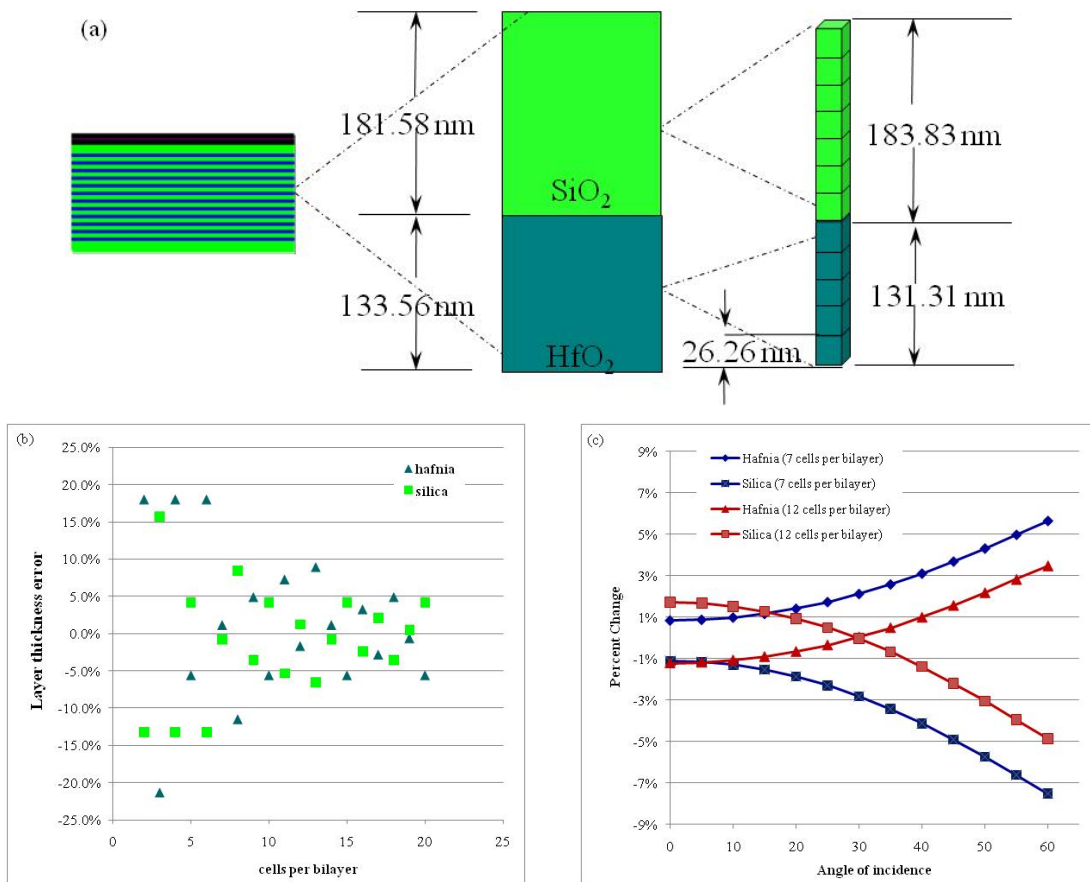


Figure 2. (a) Schematics show the discretization of layer structure and the difference between the actual thickness and the gridded dimension. (b) The dependence of error in layer thickness due to gridding at normal incidence. (c) The dependence of the percent change of layer thickness due to gridding on incident angles for 7 and 12 cells per bilayer. The 12 cell-per-bilayer case on average gives a smaller change in layer thickness.

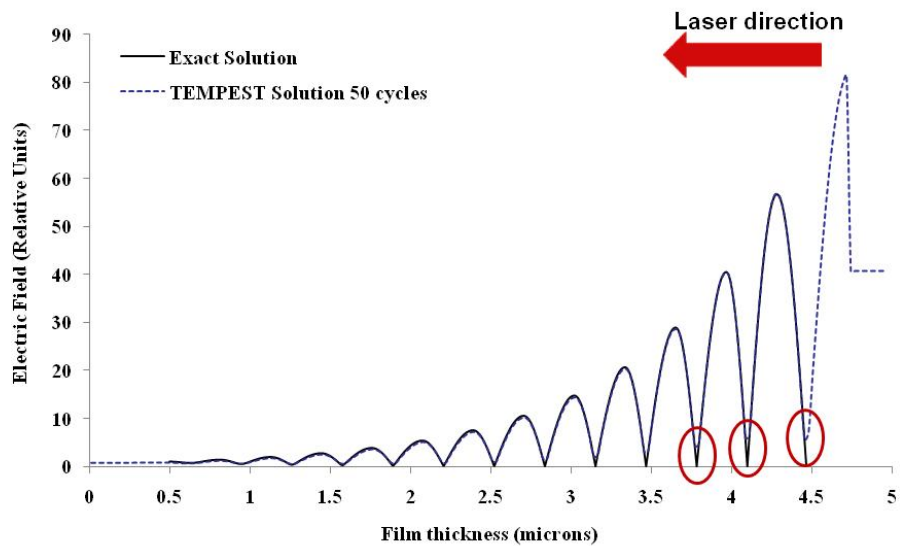


Figure 3. Comparison of the electric field distribution within a perfect stack between results obtained by simulation and that of analytic solution.

There are very few nontrivial analytic or semi-analytic test cases to benchmark against the TEMPEST code. An earlier code validating effort⁸ compared the Mie's solution¹⁷ for a plane wave interacting with a dielectric sphere to the simulation result for a spherical solid inclusion embedded within multilayers. The axial values of $|\mathbf{E}|^2$ from both methods agreed very well. Currently, we further benchmark the code by comparing the field distribution of a perfect QWOT stack obtained from the simulation against that of analytic solutions. The perfect stack consists of 24 alternating layers of hafnia (H) and silica (L) similar to those shown in figure 1. For the simulation, a 12-cell per bilayer was used to discretize the film thickness. The analytical solution was determined using the "The Essential Macleod" program. The field intensity distribution along the film depth (upon normal irradiation) determined from both methods is shown in figure 3. Because of the scale difference, the intensity spectrum obtained from the simulation was normalized by matching the maximum peak intensity to that obtained analytically. Spectrum from the simulation (dotted line) agrees well with that from the exact solution (solid line) except for the minimum values at the near surface regions (see plot inside the red circles in the figure 3) where a noticeable difference can be seen. However this discrepancy in the minimum peaks is smaller than 1% and can be suppressed by increasing the cell numbers during simulation (i.e., reduce the cell thickness). Nevertheless, because only the accuracy of maximum peak values is relevant, the observed errors at the minimum peak can be tolerated. In addition, such agreement between the two spectra is also observed for light irradiated at oblique angles of incidence (data not shown). Thus the simulation code is valid to determine the field distribution within the multilayer coatings.

3. RESULTS AND DISCUSSION

An example of the simulated E-field distribution for a defective multilayer with a 30° conical pit at 10° of incident angle is shown in Figure 4. The intensification strength is illustrated by the color scheme where larger color scale value indicates higher intensification. In general, hot spots are observed in both hafnia and silica layers and in most cases, the maximum intensification is seen at the layers near the interface. For the case shown in the figure, the maximum intensification resides in the silica layer. The field distribution along the vertical direction where peak intensification located is shown in figure 5b. The plot shows that the field strength attenuates through the film depth. It should be noted that the correlation between damage threshold and maximum intensification may not be the same for the silica layers and hafnia layers. Furthermore, previous work has shown that the damage often occurs in the hafnia layers.¹⁸ Thus in the following sections, we will focus our discussion on the simulation results for the hafnia layers.

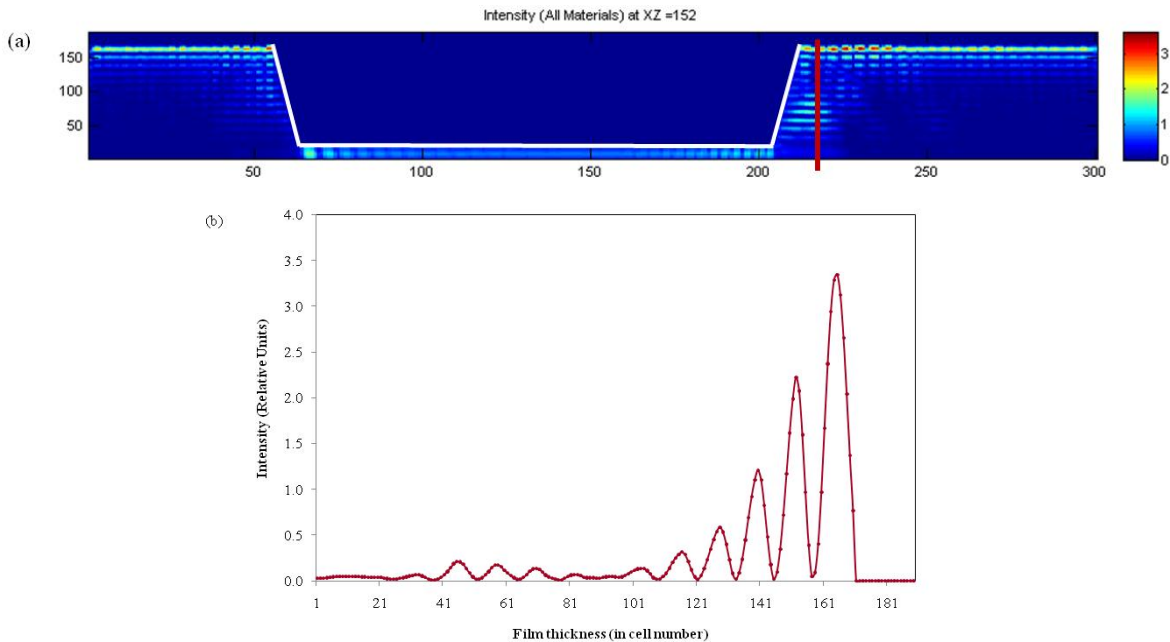


Figure 4. (a) An example of the electric field distribution within the multilayer structure obtained by TEMPESTpr2 code. Higher color scale value corresponds to higher field enhancement. For view purpose, the image is stretched along vertical direction. (b) Field strength profile along film depth as outlined in (a) by the colored line.

Pictures in figure 5 show the field distribution of the multilayer film with several different cone angles, but at a fixed 15° incidence angle. Similar to the case shown in figure 4, the hot spots are mostly located at the near surface regions (maximum peak locations are encircled in red). Assuming laser damage in films is directly correlated with field intensification, the simulation results are then consistent with experimental observations as reported previously.¹⁸ Secondly, the magnitude of the maximum intensification strongly depends on the cone angle. For example, for light irradiated at 15°, a defect with cone angle of 60° will generate a maximum intensification of ~7.0 (figure 5d) while the intensification only reaches to ~2.0 when the cone angle is at 30° (figure 5b). An intensity value of 1 or smaller indicates no field intensification.

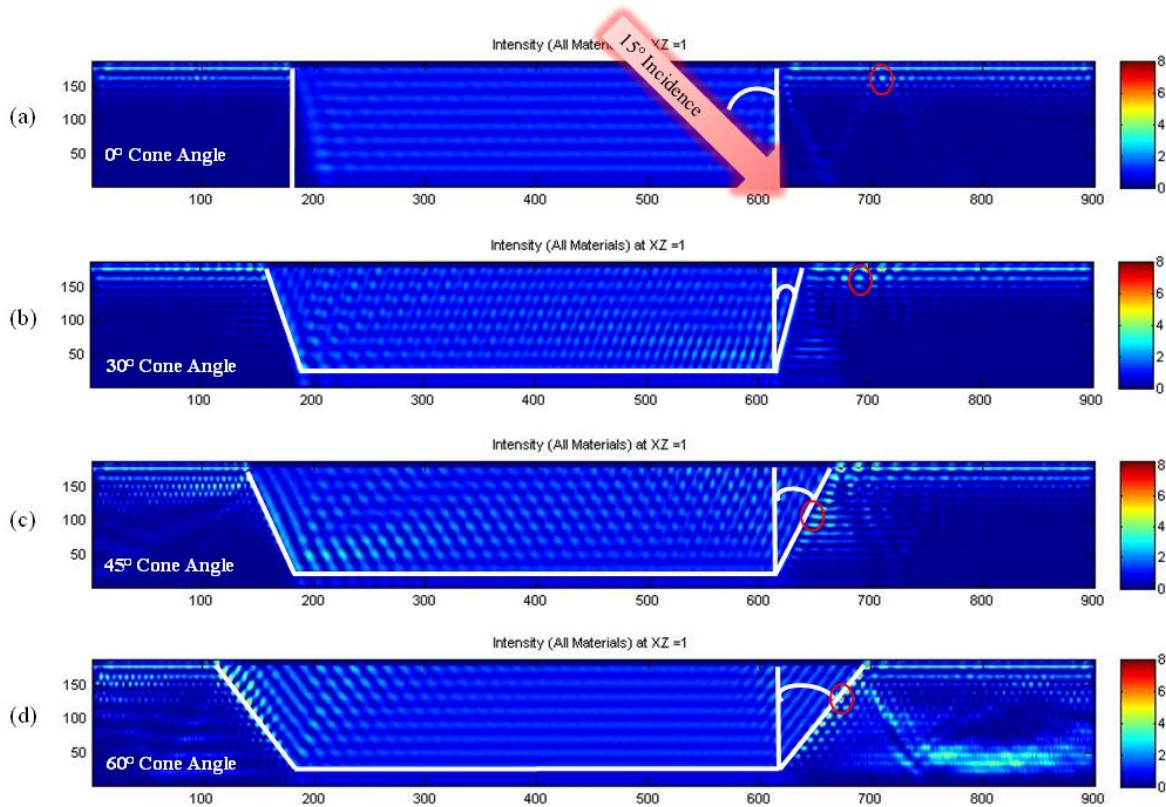


Figure 5. Representative images of simulated field distribution for multilayer film with a conical pit of different cone angles all at 15° incidence angles. Domain dimension: 90 μm x 4.963 μm . For view purpose, all images are stretched along vertical direction.

Simulations also show, for a fixed defect shape, the field distribution and the intensification magnitude are both strongly dependent on the angle of incidence. For example, for a 45° conical pit, at normal incidence, the maximum field intensification is over ~9 times the base value. The intensification only reaches 2, however, when light impacts the multilayer thin film at 60°. For all the incident angles simulated, the maximum intensification varies from ~1.9 to ~9.3. Figures 6a-d illustrate the field distribution and enhancement within the multilayer film due to the 45° conical pit for incident angles of 0°, 15°, 30°, and 60°. Beside the wide spread magnitude in maximum intensification, the field distribution or standing-wave pattern within the film is also quite different for each beam incident angle.

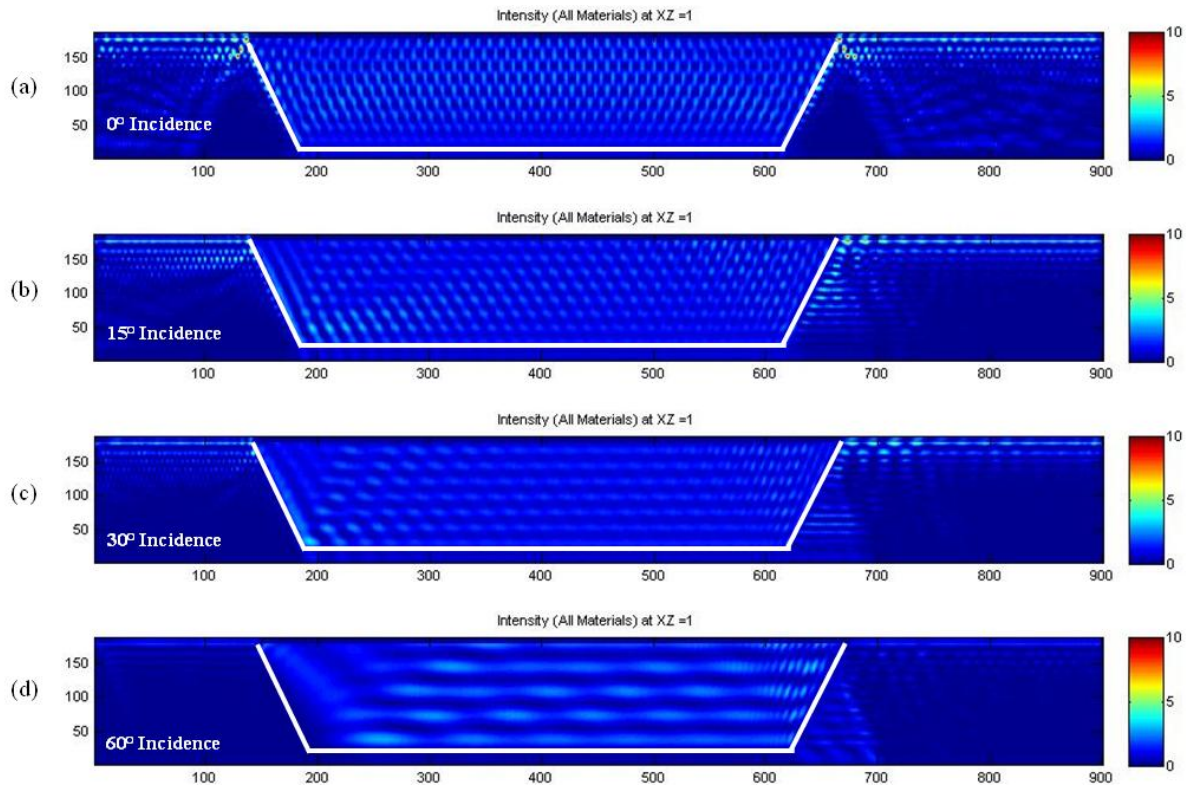


Figure 6. Representatives of simulated field distribution for multilayer film with a conical pit of 45° cone angle at a series of beam irradiation angles. Domain dimension: $90 \mu\text{m} \times 4.963 \mu\text{m}$. For view purpose, all images are stretched along vertical direction.

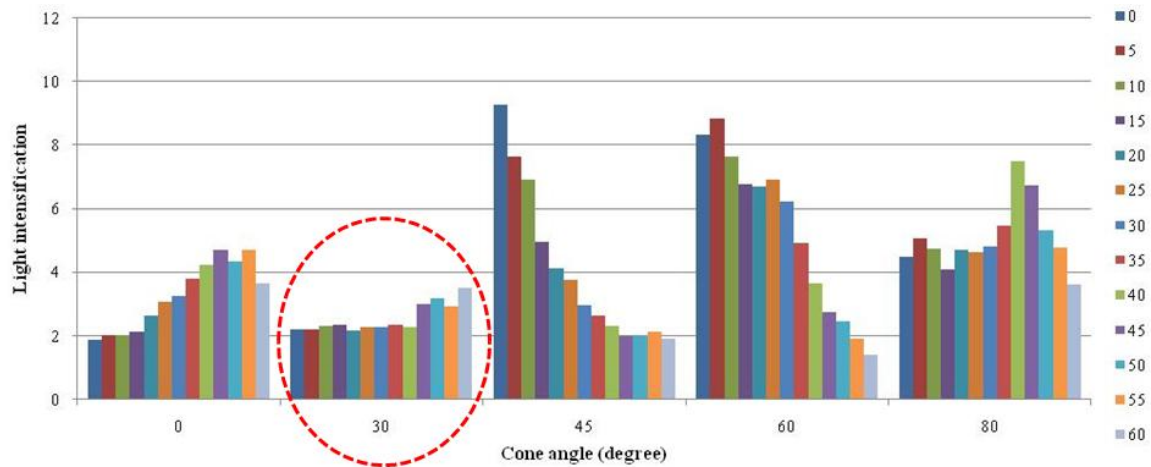


Figure 7. Summary plot shows the distribution of the maximum intensification within defective multilayer film for various cone angles and a series of angles of incidence. The red dotted circle indicates that a 30° conical pit generates the least amount of field intensification for all incidence angles. The color-box legend indicates the angle of incidence

In figure 7, the maximum magnitude of the intensification within the hafnia layer for the defective multilayer is plotted at different cone angles for a range of incident angles. The cone angles for the simulations are 0° , 30° , 45° , 60° , and 80° and the angle of incidence ranges from 0° to 60° in 5° increments. In general, for a given cone angle, the maximum intensification values varies strongly with the angle of incidence. The dependence on incidence angles, in most cases,

can be described by a monotonic function. On the other hand, for a given light irradiation direction, the dependence of the maximum intensification on cone angles is rather complex and does not follow a monotonic fashion.

It is apparent that the conical pit with a 30° cone angle generates the least amount of field enhancement on average within the multilayer for light irradiated at all incidence angles. Cylinders (zero degree cone angle) also tend to have lower intensification than cones with cone angles exceeding 30° . The results show that electric field intensification is minimized for shallower cones and suggest that potential mitigation features should have shallow ($< 30^\circ$) conical angles to improve mirror laser damage resistance.

We have also observed an interesting phenomenon where the defective multilayer film exhibits a wave guide property. Such effect is especially prominent for cylinders (cones with zero degree of cone angle). As shown in figure 8, the wave guide generates a periodic maximum intensification spot at both shallow and deep regions within the multilayer. While the reflection point at the shallow region reaches a peak intensification of ~ 5 , the intensification at the deeper reflection point is also as high as ~ 3.5 . Field intensification at the deep location may be responsible for the observed deeper damage site within the coating multilayers in the transport or polarized mirrors. Our results suggest an alternative source of field intensification within the film especially for those spots located in deeper region of the multilayer film.

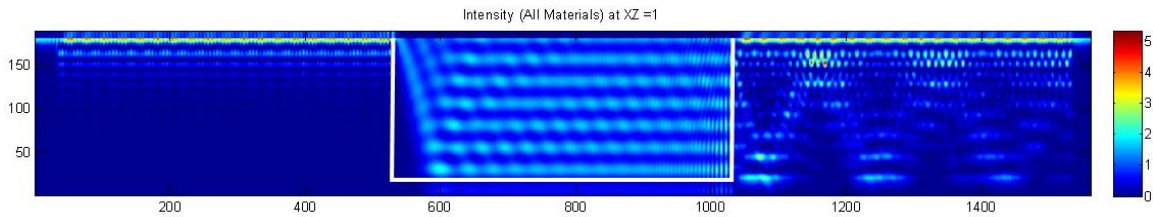


Figure 8. Simulation image showing a wave guide effect generated within multilayer film for a zero angle cone at 45° irradiation angle. The high intensification points clearly show at the right side of the film in both shallow and deep regions with an apparent periodicity. Domain dimension: $150 \mu\text{m} \times 4.963 \mu\text{m}$. For view purpose, all images are stretched along vertical direction.

4. SUMMARY

We have found that, through simulation, electric field intensification within the defective multilayer film depends on both the cone angle and the angle of incidence of the impinging light. Specifically, for a given incident angle, the dependence on the cone angle is rather complex and does not follow a simple rule. For a cone with a fixed cone angle, the dependence on the incidence angle, however, follows a simple pattern although the function may be different for each cone angle. Overall, our results show that conical defects with shallow cone angle ($\leq 30^\circ$) generate the least amount of intensification for light irradiated at all incident angles. Therefore an optimal (or high fluence) conical mitigation feature should have shallow ($< 30^\circ$) conical angles. In addition, when certain conditions such as incident angle, cone angle, and index of refraction are met, a waveguide generated within the film can also be a source of intensification. The waveguide effect not only causes intensification near the top surface but also at the much deeper locations. Further studies are needed to experimentally verify the presence of the waveguide within the multilayer film and to reveal the underlying mechanism by which waveguides form within the multilayer film at the presence of mitigation defects.

5. ACKNOWLEDGEMENT

This work was performed under the auspices of the U.S. Department of Energy by Lawrence Livermore National Laboratory under Contract DE-AC52-07NA27344. This document was prepared as an account of work sponsored by an agency of the United States government. Neither the United States government nor Lawrence Livermore National Security, LLC, nor any of their employees makes any warranty, expressed or implied, or assumes any legal liability or

responsibility for the accuracy, completeness, or usefulness of any information, apparatus, product, or process disclosed, or represents that its use would not infringe privately owned rights. Reference herein to any specific commercial product, process, or service by trade name, trademark, manufacturer, or otherwise does not necessarily constitute or imply its endorsement, recommendation, or favoring by the United States government or Lawrence Livermore National Security, LLC. The views and opinions of authors expressed herein do not necessarily state or reflect those of the United States government or Lawrence Livermore National Security, LLC, and shall not be used for advertising or product endorsement purposes.

*Address correspondence to S. Roger Qiu, Lawrence Livermore National Laboratory, 7000 East Avenue, L-491, Livermore, CA 94551. Email: qiu2@llnl.gov. Phone: (925) 422-1636.

REFERENCES

- [1] J. DiJon, T. Poiroux, C. Desrumaux, "Nano absorbing centers: a key point in the laser damage of thin films", Proc. SPIE 2966, 315-325 (1997).
- [2] F.Y. Genin, C.J. Stolz, "Morphologies of laser -induced damage in hafnia-silica multilayer mirror and polarizer coatings", Proc. SPIE 2870, 439-448 (1996).
- [3] J. Dijon, P. Garrec, N. Kaiser, U.B. Schallenberg, "Influence of substrate cleaning on LIDT of 355 nm HR coatings", Proc. SPIE 2966, 178-186 (1997).
- [4] Justin E. Wolfe, S. Roger Qiu, Chris J. Stolz, "Laser damage resistant features in dielectric coatings created by femtosecond laser machining", Proc. SPIE, submitted (2009).
- [5] P. Geraghty, W. Carr, V. Draggoo, R. Hackel, C. Mailhiot, M. Norton, Proc. SPIE 6043, Q4030 (2007).
- [6] M. Tricard, P. Dumas, J. Menapace, "Continuous phase plate polishing using Magnetorheological Finishing", Proc. SPIE 7062, V1-V8 (2008).
- [7] P.W. Baumeister, "Optical coating technology", SPIE (2004), Chaps. 5-51.
- [8] C. J. Stolz, M.D. Feit, T.V. Pistor, "Laser intensification by spherical inclusions embedded within multilayer coatings", Applied Optics 45 (7), 1594-1601 (2006).
- [9] A. Wong, "rigorous three-dimensional time-domain finite-difference electromagnetic simulation", Ph.D. dissertation, University of California at Berkeley, Berkeley, California (1994).
- [10] T.V. Pistor, "electromagnetic simulation and modeling with applications in lithography", Ph.D. dissertation University of California at Berkeley, Berkeley, California (2001).
- [11] K.S. Yee, "Numerical solution of initial boundary value problems involving Maxwell's equations in isotropic media", IEEE Trans. Antennas Propag. 14, 302-307 (1996).
- [12] J. Berenger, "A perfectly matched layer for the absorption of electromagnetic waves", J. Comp. Phys. 114, 185-200 (1994).
- [13] C.J. Stolz, S. Hafeman, T.V. Pistor, "Light intensification modeling of coating inclusions irradiated at 351 and 1053 nm", Applied Optics 47 (13), (2008).
- [14] C.J. Stolz, F.Y. Genin, T.V. Pistor, "Electric field enhancement by nodular defects in multilayer coatings irradiated at normal and 45° incidence", Proc. of SPIE 5273, 41-49 (2004).
- [15] F.Y. Genin, A. Salleo, T.V. Pistor, L.L. Chase, "Role of light intensification by cracks in optical breakdown on surfaces", J. Opt. Soc. Am. A 18 (10), 2607-2616 (2001).
- [16] The Essential Macleod. Thin film Center Inc., 2745 Via Rotonda, Tucson, AZ 85716, USA.
- [17] G. Mie, "Beitraege Zur Optik Trueber Medien, Speziell-Kolloidaler Metalosungen" Ann. Physik 25, 377-445 (1908).
- [18] D.H. Gill, B.E. Newnam, J. McLeod, "Use of non-quarter-wave designs to increase the damage resistance of reflectors at 532 and 1064 nanometers". In Glass AJ, and Guenther AH (eds) Laser-Induced Damage in Optical Materials: NBS SP 509 260-270 (1977).